ADVANCED OPTICAL MATERIALS
www.advopticalmat.de

All-Dielectric Metamaterial Fabrication Techniques

Ke Bi, Qingmin Wang, Jianchun Xu, Lihao Chen, Chuwen Lan, and Ming Lei**

All-dielectric metamaterials with low loss are a rapidly developing research hotspot in the field of metamaterials, and offer additional design freedom for electromagnetic devices. Many types of fabrication techniques are used to prepare all-dielectric metamaterials, so as to realize specific physical properties. A key to efficient electromagnetic manipulation is the proper choice of the fabrication technique, which enables the all-dielectric metamaterials to be easily coupled to integrated devices. Here, an overview of existing fabrication techniques for all-dielectric metamaterials is provided. Based on material compositions and accuracy requirements, typical fabrication methods for microwave, terahertz, and optical all-dielectric metamaterials are discussed. In addition, the advantages and disadvantages of each fabrication method are outlined. This comparative analysis of all-dielectric metamaterial fabrication techniques will be valuable for the design of novel all-dielectric metamaterials with desired physical properties, thereby expanding the scope of their applications.

1. Introduction

Metamaterial is a type of artificial material in which the electromagnetic properties are mainly defined by the unit cells, with a feature size much smaller than the operational wavelength.[1–3] A metamaterial exhibits many novel electromagnetic properties, such as negative refraction, an inverse Doppler effect, and backward Cherenkov radiations, and has many important potential applications.[4–7] Pendry et al. realized the negative permeability by using split-ring resonators;[8] today, most current metamaterials are constructed using periodic artificial metallic structures.[9–11] Although metamaterials exhibit exotic physical properties and have a wide range of potential applications, metallic metamaterials have many unsolved problems and/or bottlenecks, such as serious Ohmic loss and narrow bandwidths.[12,13]

Recently, there has been a great deal of attention devoted to all-dielectric metamaterials, which have a wide range of potential applications in wave front control,[14,15] absorbers,[16] strong-field-enhanced spectroscopy,[17] and perfect reflectors,[18,19] at frequencies ranging from the low microwaves to the optical region. Basically, all-dielectric metamaterials are composed of polymers, dielectrics, ferrites, or composite materials.[20–22] The unusual electromagnetic properties of all-dielectric metamaterials not only derive from their artificial structure, but also originate directly from the materials, revealing an approach to designing metamaterials with more freedom.[23]

Since the initial proposal of all-dielectric metamaterials, various realization mechanisms have been studied and reported.[24–26] The most classical mechanism is based on the so-called Mie-resonance theory, and has been studied extensively.[27–29] In this strategy, dielectric particles with relatively high permittivity are used to generate strong magnetic or electric resonance through electromagnetic wave interaction. Therefore, a negative permeability or permittivity can be produced by the oscillation of the resulting magnetic or electric dipole. This mechanism is simple and versatile, and is generally adopted for the realization of all-dielectric metamaterials with low losses.[30] Ferromagnetic resonance (FMR) theory is another classical realization mechanism for all-dielectric metamaterials.[31,32] When the ferromagnetic resonance of the ferrite takes place, a negative permeability appears. Many factors can influence the FMR of the magnetic materials, including the bias magnetic field, magnetocrystalline anisotropy field, and demagnetization field. Hence, ferrite metamaterials with dual-band, multi-band, or tunable properties can be obtained, providing a way to resolve the narrow band problem. Besides, mechanisms such as indefinite media or crystal lattice vibration have also been used to realize all-dielectric metamaterials.[33,34]

When determining the realization mechanism for an all-dielectric metamaterial, one crucial factor must be considered: the choice of a fabrication method. Moreover, to achieve different performances, many types of materials with specific electromagnetic properties are used to prepare all-dielectric metamaterials.[35] Hence, researchers have developed various techniques for the fabrication of all-dielectric metamaterials derived from different materials.[36–40] In addition, the fabrication requirements are quite different for all-dielectric metamaterials operating at frequencies ranging from the microwave to optical regions. In particular, the size of the metamaterial unit cell is much smaller than the operational wavelength, making the fabrication technology for all-dielectric metamaterials become the key to their further application. Here, we present a comprehensive review of the various techniques used to produce all-dielectric metamaterials. We review the existing fabrication technologies for microwave, terahertz, and optical all-dielectric

Dr. K. Bi, Dr. Q. Wang, Dr. J. Xu, Dr. L. Chen, Dr. C. Lan, Prof. M. Lei
State Key Laboratory of Information Photonics and Optical Communications
School of Science
Beijing University of Posts and Telecommunications
Beijing 100876, China
E-mail: lanchuwen@bupt.edu.cn; mlei@bupt.edu.cn

The ORCID identification number(s) for the author(s) of this article can be found under https://doi.org/10.1002/adom.202001474.

DOI: 10.1002/adom.202001474

metamaterials, respectively, according to different working frequencies and accuracy requirements. This article also highlights some of the advantages and disadvantages of each fabrication technology. In addition, this review includes schematic diagrams for the various methods of all-dielectric metamaterial production, and for the features of the all-dielectric metamaterials that can be produced using each technique.

2. Microwave All-Dielectric Metamaterial Fabrication Techniques

Microwave devices have wide applications in information transmission field, such as radar and communications. All-dielectric metamaterials with an extraordinary electromagnetic response and low dielectric loss in the microwave range are desirable for developing electromagnetic devices. Therefore, many efforts have been devoted to the fabrication of microwave all-dielectric metamaterials. Owing to the limitations of the operating wavelength and fabrication technology, the size of the all-dielectric metamaterial for microwaves is mainly within the millimeter range. In this section, the methods for fabricating all-dielectric metamaterials are classified as follows.

2.1. Molding–Sintering Method

A ceramic with relatively high permittivity is beneficial to producing an electromagnetic response in the microwave range. Therefore, ceramics have been extensively used to fabricate all-dielectric metamaterials. The molding–sintering method is a specific technology for fabricating all-dielectric metamaterials based on ceramics. In the basic production process of the molding–sintering method as reported by Yahiaoui et al.,[41] a ceramic powder precursor was prepared using compressing molding method, in which pure commercial titanium dioxide (TiO_2) powders were pressed into cylinder blocks. Then, the pre-fabricated pellets were sintered into ceramics at a high temperature (1300 °C). **Figure 1**a shows the process flow for the fabrication of all-dielectric metamaterials using the molding–sintering method. The fabricated ceramic pellets (Figure 1b) are placed in periodic holes in a Rohacell substrate (Figure 1c) to obtain the all-dielectric metamaterial, which can simultaneously realize the left-handed property and broadband magnetic response.

Ceramic with other shapes can also be prepared for fabricating all-dielectric metamaterials using this method. A rectangular ceramic was prepared by pressing $0.7Ba_{0.6}Sr_{0.4}TiO_3$-$0.3La(Mg_{0.5}Ti_{0.5})O_3$ powders into rectangular blocks, and then sintering to ceramics at 1500 °C. The obtained rectangular ceramic particles were then arranged in a supporting matrix produced by a 3D printer to construct the all-dielectric metamaterials. The fabricated all-dielectric metamaterial frequency-selective surfaces can achieve broadband stopband.[42] A cross-shaped ceramic sample was fabricated by pressing $0.7Ba_{0.6}Sr_{0.4}TiO_3$-$0.3La(Mg_{0.5}Ti_{0.5})O_3$ powders into a cross-shaped mold. A supporting matrix with cross-shaped holes was prepared by a 3D printer.[43] The all-dielectric metamaterial frequency-selective surface based on the cross-shaped ceramic can realize a reconfigurable electromagnetic response by changing the orientation of the metamaterial.

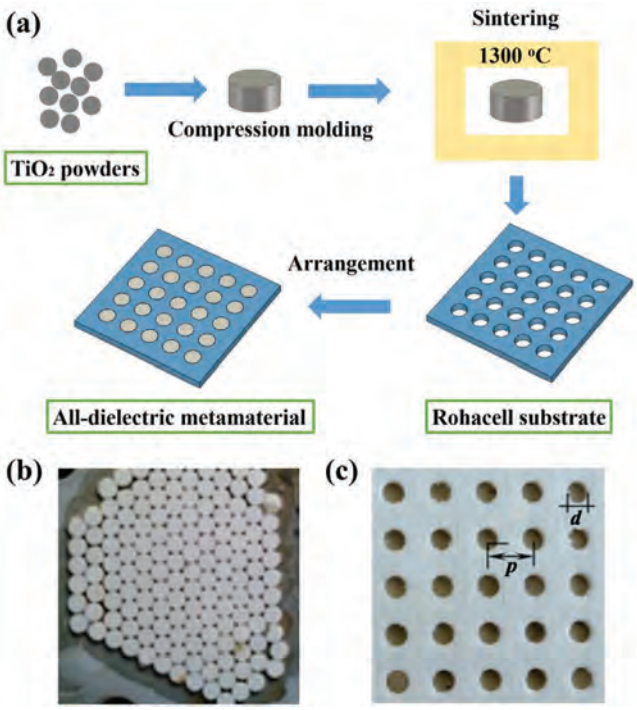

Figure 1. a) Process flow for the fabrication of all-dielectric metamaterial with molding–sintering method. b) Photograph of the fabricated TiO_2 disks. Reproduced with permission.[41] Copyright 2012, AIP Publishing. c) Photograph of the Rohacell substrate. Reproduced with permission.[41] Copyright 2012, AIP Publishing.

2.2. Cutting–Molding Method

The cutting–molding method is another technology for fabricating all-dielectric metamaterials based on ceramics. This method can produce many samples at once. In an example of the basic production process of the cutting–molding method, a $Ba_{0.5}Sr_{0.5}TiO_3$ doped 10 wt% magnesia (MgO) ceramic plate with a thickness of 1 mm was fabricated using a tape casting technique, and was sintered at 1400 °C. Then, the ceramic plate was cut into cuboids, each with a size of $2 \times 2 \times 1$ mm^3. Finally, the all-dielectric metamaterial was obtained by embedding the ceramic cuboids into a Teflon slab matrix with periodic holes.[44] The process flow for the fabrication of an all-dielectric metamaterial using the cutting-molding method is shown in **Figure 2**a. The fabricated ceramic cuboids are shown in Figure 2b. As shown in Figure 2c, the all-dielectric metamaterial is a flat lens, providing refocusing and omnidirectional radiation properties.

This method is suitable for fabricating an all-dielectric metamaterial with many samples, and is widely used to fabricate all-dielectric metamaterials.[45–49] In addition to the ceramic plates produced by the tape casting technique, ceramics made by other methods can also be cut and molded to fabricate all-dielectric metamaterials. As reported by Bi et al.,[50] a special ferrite ceramic was cut into dimensions of $1 \times 1 \times 10$ mm^3 and inserted into a Teflon substrate to fabricate a magnetically

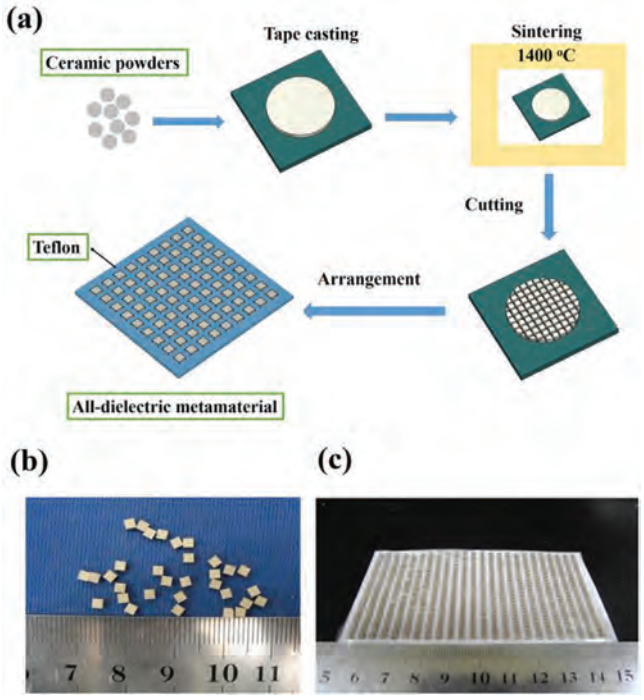

Figure 2. a) Process flow for fabrication of all-dielectric metamaterial with cutting–molding method. b) Photograph of ceramic cuboids. Reproduced with permission.[44] Copyright 2013, Optical Society of America. c) Photograph of all-dielectric metamaterial based on ceramic cuboids. Reproduced with permission.[44] Copyright 2013, Optical Society of America.

tunable all-dielectric metamaterial. The process flow and a photograph of the ferrite rods are shown in **Figure 3**a. A fabricated all-dielectric metamaterial filter based on the ferrite rods has a strong resonance, and a tunable bandwidth and operating frequency. Figure 3b shows the fabricated magnetically tunable all-dielectric metamaterial bandstop filter. Figure 3c shows a magnetically tunable all-dielectric metamaterial bandpass filter fabricated by combining two ferrite rods with different saturation magnetizations.

In addition, the cutting ceramic particles can also be combined with other-shaped particles to fabricate all-dielectric metamaterials. In the study by Li et al.,[51] an H-shaped sample has been prepared for all-dielectric metamaterial band-pass frequency-selective surfaces with low loss.

2.3. Cavity Injection Method

The cavity injection method is mainly used to fabricate all-dielectric metamaterials based on liquid. In the microwave range, water behaves with dielectric properties, and is an ideal material for low-cost, environmentally friendly, and easily obtained all-dielectric metamaterials.[52–54] All-dielectric metamaterials based on water have been realized using the cavity injection method.[55,56]

As shown in **Figure 4**a, the metamaterial is prepared by injecting water into glass tubes in a Plexiglas box. Figure 4b shows a photograph of an all-dielectric metamaterial based on water. The all-dielectric metamaterial based on water has a transmission aspect related to the strong toroidal mode.[57]

An all-dielectric metamaterial based on water can realize ultra-wideband absorption.[58] In one study, a ultraviolet-light photosensitive resin (UV-PR) substrate with cross water-flow channels was fabricated using a 3D printer. The UV-PR was used to surround four sides of a sample, to encapsulate the sample. An inlet and outlet were reserved on the upper and lower sides of the sample, respectively. In addition, all-dielectric metamaterials have wideband absorption, which has potential applications in electromagnetic stealth. For example, a flexible water container for supporting water was fabricated using 3D printing technology and a thermoplastic urethane material. This flexible all-dielectric metamaterial based on water could realize ultra-wideband absorption with a 4 mm thickness.[59]

Room-temperature ionic liquids are new flexible materials and act as green electrolytes as they are molten organic salts consisting of anions and cations. The ionic liquids have excellent performances in regards to thermal stability,[60] the liquid temperature range,[61,62] recyclability,[63] and ionic conductivity.[64–66] Moreover, the ionic liquids have high dielectric-loss factors in the microwave range, which are desirable for fabricating microwave all-dielectric metamaterials.[67] The cavity injection method has been used to fabricate all-dielectric metamaterials based on ionic liquids. In one example, a 3D printer was employed to fabricate hollow annular groove unit cells. A whole annular groove bracket with dimensions of 180×180 mm^2 was combined with the annular groove unit cells. The ionic liquids were injected into the hollow of the annular groove using injectors, and the hollow was covered the hollow by a lid. An all-dielectric metamaterial based on ionic liquids can realize ultra-wideband absorption with insensitive polarization and oblique incidence properties.[68]

2.4. Drilling Method

Drilling methods are used to prepare all-dielectric metamaterials composed of composite materials with low hardness. The employed composite materials are fabricated by dispersing high-permittivity dielectric fillers into polymers with low permittivity. Then, sub-wavelength holes are drilled in the obtained composite materials for the unit cells of the metamaterial. The composite material is low-loss, flexible, and light, and is therefore suitable for the fabrication of an all-dielectric metamaterial with low permittivity.[69] In one study, a multilayered polytetrafluoroethylene (PTFE) and glass fiber (F4B) with a dielectric constant of 2.65 and a loss tangent of 0.001 was used to fabricate an all-dielectric cloak. The thickness of the employed F4B was 1 mm. According to the design, the location and diameter of the drilled holes were determined so as to achieve the cloaking property. The cloak could conceal objects in the microwave band with wideband transmission and low loss.[70]

In another study, a conventional melt blending method was used to produce a composite dielectric plate by embedding TiO_2 in a polypropylene (PP) matrix. To reduce the moisture, the purchased TiO_2 and PP were dried at 50 °C overnight. When the PP melted at 180 °C, the TiO_2 was added into the PP, and was mixed until uniformly blended. The trapped air in the mixture was pulled away by evacuating the mixer. The homogenized composite materials were poured at 140 °C to produce

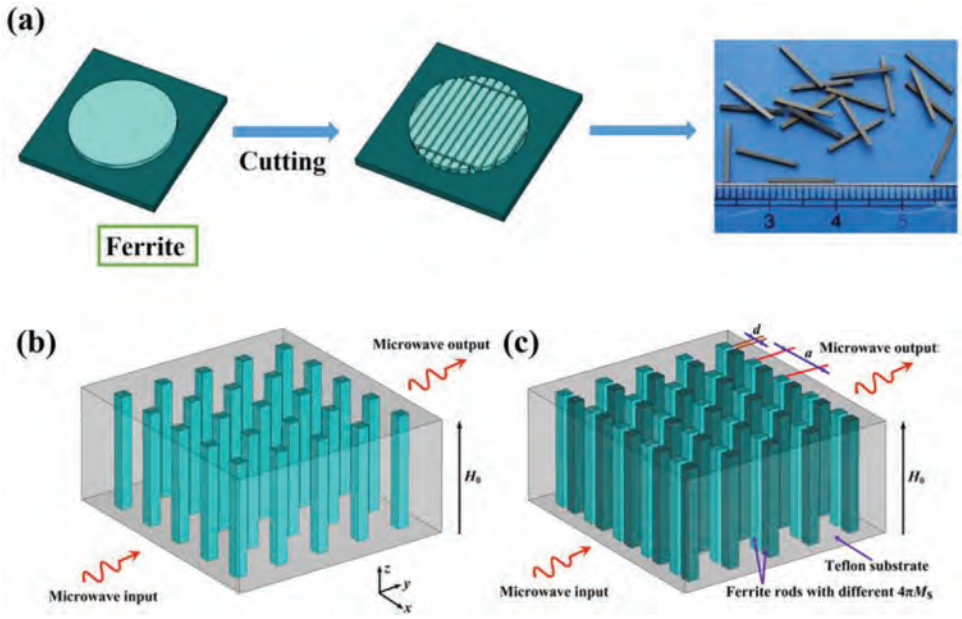

Figure 3. a) Process flow for fabrication of ferrite rods. b) Magnetically tunable all-dielectric metamaterial bandstop filter based on ferrite rods. Reproduced with permission.[50] Copyright 2015, AIP Publishing. c) Magnetically tunable all-dielectric metamaterial bandpass filter based on ferrite rods. Reproduced with permission.[50] Copyright 2015, AIP Publishing.

the final dielectric plate. The all-dielectric metamaterial was constructed by uniformly drilling via-holes with specific diameters on the composite dielectric plate. An all-dielectric metamaterial lens could be produced using the drilled-hole PP/TiO_2 composite materials.[71] **Figure 5**a shows the process flow for the fabrication of a composite material based on an all-dielectric metamaterial with a drilling method. Figure 5b shows the fabricated all-dielectric metamaterial, with via-holes of different sizes. The size of the hole can affect the permittivity of the all-dielectric metamaterials. In addition, fillers with high permittivity for TiO_2 can be used instead of carbon graphene, nanotubes, and other dielectric nanoparticles.[72–76] The matrix polymer PP can be replaced by polystyrene (PS), polyethylene (PE), PTFE, or thermoset resins.[77–79] The processing conditions, such as the shape and size of the fillers, the combined types of the composite materials, and the fabrication process, can influence the performance of the fabricated composite materials.

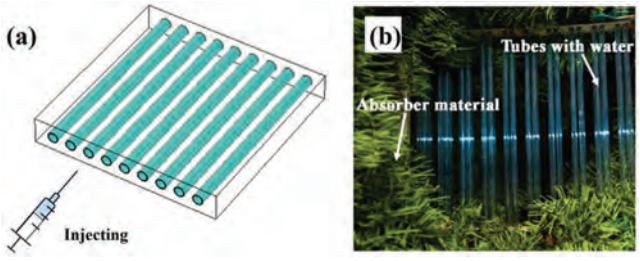

Figure 4. a) Schematic diagram of the all-dielectric metamaterial based on water using cavity injection method. b) Photograph of all-dielectric metamaterial based on water. Reproduced with permission.[57] Copyright 2017, Springer Nature.

2.5. Templated Self-Assembly Method

A new templated self-assembly method has been proposed for fabricating all-dielectric metamaterials with negative permittivity and low dielectric loss. After a process of self-assembly

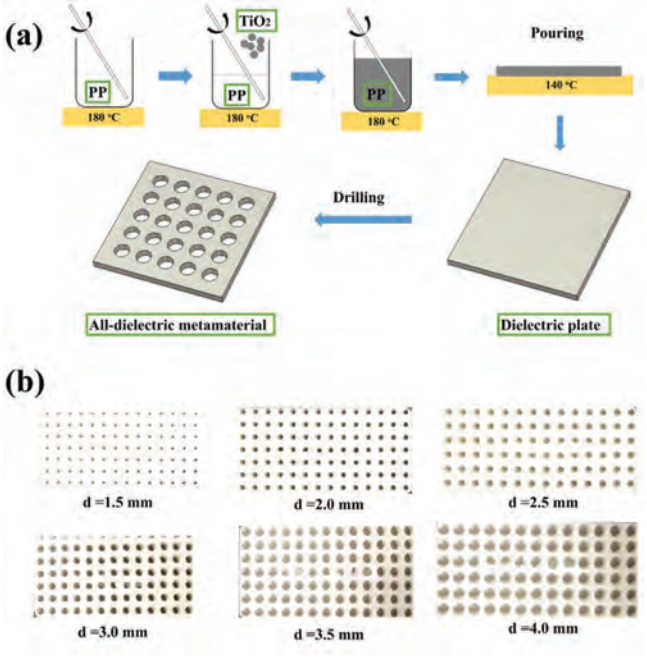

Figure 5. a) Process flow for fabrication of composite material based all-dielectric metamaterial with drilling method. b) Photograph of all-dielectric metamaterial with via-holes of different sizes. Reproduced with permission.[71] Copyright 2017, Elsevier.

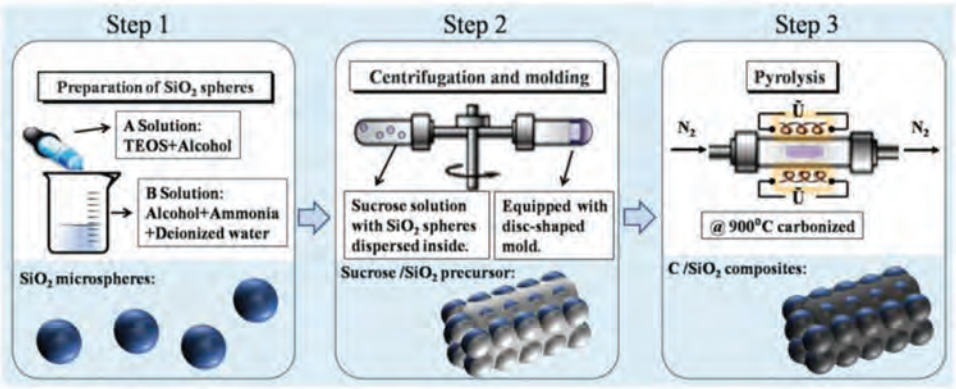

Figure 6. Process flow for fabrication of all-dielectric metamaterial with templated self-assembly method. Reproduced with permission.[80] Copyright 2018, Royal Society of Chemistry.

and pyrolysis, a 3D carbon network is constructed in a silica spherical matrix, and can realize a stable radio-frequency negative permittivity. The templated self-assembly method expands the metamaterial design freedom. This metamaterial operates at the microwave frequencies due to its artificial structure. The process flow for fabrication of an all-dielectric metamaterial with the templated self-assembly method is shown in **Figure 6**. In step 1, monodispersed SiO_2 (silica) microspheres are prepared by adding solution A (with orthosilicate (TEOS) and alcohol) to solution B (with alcohol, ammonium, and deionized water). The monodispersed SiO_2 microspheres are finally obtained by centrifuge separation, cleaning, and drying processes. In step 2, SiO_2 spheres suspension is obtained by adding the pre-prepared monodispersed SiO_2 microspheres to sucrose solutions, and ultrasonically dispersing them. After centrifugal molding and drying, cylindrical sucrose/SiO_2 precursor samples are obtained. The final C/SiO_2 composite-based metamaterial is obtained via a pyrolysis process.[80]

A comparison of the fabrication techniques for microwave all-dielectric metamaterials is shown in **Table 1**. It summarizes the five fabrication methods for the microwave all-dielectric metamaterials: the molding–-sintering method, cutting–molding method, cavity injection method, drilling method, and templated self-assembly method. The molding–-sintering method is used to fabricate an all-dielectric metamaterial based on ceramics. The operating frequency of the metamaterial can be adjusted by changing factors such as the types of ceramic precursors, proportions, and fabrication conditions. However, this method has difficulty in fabricating many samples at once. Moreover, the fabricated metamaterials usually have a narrow band for the strong electromagnetic response. The cutting–molding method is another technology for fabricating the all-dielectric metamaterials based on ceramics. Compared to the molding–sintering method, this method can produce many samples at once. The cavity injection method is mainly used to fabricate an all-dielectric metamaterial based on liquid. It is a simple and low-cost method for fabricating an all-dielectric metamaterial with wideband and high-efficiency properties. However, the metamaterials fabricated by this method always have a limited application, owing to their high dielectric loss in the microwave range. The drilling method is a simple method for fabricating an all-dielectric metamaterial. However, the metamaterials fabricated by this method always have low permittivity, limiting their application in the microwave range.

Table 1. Comparison of fabrication techniques for microwave all-dielectric metamaterials.

Method	Material	Temperature [°C]	Size	Frequency range [GHz]	Bandwidth [GHz]	Ref.
Molding–sintering	TiO_2	1300	3.3 mm	30–70	5.0	[41]
	BST/$La(Mg_{0.5}Ti_{0.5})O_3$	1500	2.0 mm	8–12	1.5	[42]
Cutting–molding	BST/MgO	1400	2.0 mm	8–12	0.37	[44]
	BST	–	1.0 mm	6–12	0.34	[45]
	BST/Mn	–	0.88 mm	8–12	0.4	[46]
	$CaTiO_3/ZrO_2$	1400	2.2 mm	8–12	–	[48]
	Ferrite	–	1.0 mm	8–12	0.25	[50]
Cavity injection	Water	Room	14.0 mm	5–30	14.7	[58]
	Ionic liquid	Room	5.0 mm	10–50	36.2	[68]
Drilling	F4R/F4B	Room	1.3 mm	12.4–18	5.6	[69]
	F4B	Room	2.0 mm	8–12	4.0	[70]
	TiO_2/PP	180	1.5 mm	2.6–3.95	1.35	[71]
Templated self-assembly	C/SiO_2	900	527 nm	0–1	0.7	[80]

The templated self-assembly method can realize the negative permittivity, but the operation frequency is low.

3. Terahertz All-Dielectric Metamaterials Fabrication Methods

All-dielectric metamaterials are a promising route for building terahertz devices. In the realm of terahertz devices, silicon-based materials have been employed to realize high-performance all-dielectric metamaterials.[81–84] By changing the dielectric properties and sizes of the particles, the resonant frequency of the electromagnetic wave can be modulated.[85,86] Therefore, as compared with conventional metallic metamaterials, all-dielectric metamaterials improve the problems in absorption and energy loss, as well as the quality factor.[87]

3.1. Deep Reactive Ion Etching and Laser Micromachining Methods

Generally, the fabrication process of silicon-based all-dielectric metamaterials includes mask photolithography and deep reactive ion etching (DRIE) as shown in **Figure 7**a.[88,89] The mask photolithography is conducted to pattern the photoresist (PR) layer, thereby preparing for the further processing of the DRIE.[90,91] To realize the mask photolithography, the PR is spin-coated on a silicon wafer. By employing conventional mask photolithography, the PR layer is etched as the desired mask for the DRIE. As depicted in Figure 7b, a silicon oxide layer is usually first deposited on the silicon wafer, via plasma-enhanced chemical vapor. Then, the PR layer is spin-coated on the oxide layer. By using photolithography and dry etching, the PR layer and oxide layer are etched, to thereby act as the mask for DRIE. Owing to the excellent oxide selectivity of DRIE, this oxide mask has good protective effects in DRIE. In addition, a glass wafer or a metal layer is often bonded on the bottom of the silicon wafer, to act as a substrate. Although the metal layer can inhibit the charge accumulation on the structure bottom, it also introduces a parasitic capacitance. The glass wafer can effectively restrain the effects of footing or notching. These methods comprise improvements over traditional technology, which is helpful for the DRIE. After the DRIE process, the PR layer is removed using acetone and isopropanol, and the oxide and metal layers are leaned by piranha and hydrogen fluoride. Finally, the silicon-based all-dielectric metamaterial is peeled off and obtained, which can be used to design various devices with excellent functionality. Especially in the terahertz band, DRIE is a common fabrication method for all-dielectric metamaterials. For example, our group recently designed a highly efficient active all-dielectric metasurfaces, as shown in Figure 7c, based on DRIE technology.[92] By using this method, an all-dielectric metasurface with "hybrid structures" is obtained, and can be applied in ranges from terahertz to optic.

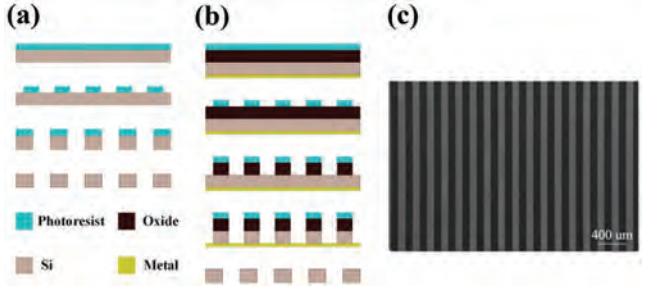

Figure 7. The fabrication process of silicon-based all-dielectric metamaterials: a) conventional method, b) adding the oxide layer and metal layer on the double sides of the silicon wafer, and c) a processed sample. Reproduced with permission.[92] Copyright 2019, American Chemical Society.

Laser micromachining combines mechanical and optical technologies to etch high-quality micro/nanostructures from many materials, and is usually used to define the surface shape of a silicon or quartz material.[93] Laser micromachining technology has been widely applied in material fabrication in the optic to microwave range, owing to its distinct advantages such as its clean ablative etching, simple steps, and compatibility with lithographic processes. During the DRIE processes, the desired masks are often made by laser micromachining. In the laser micromachining setup, the laser is focused onto the sample using a lens. The ultrahigh temperature directly transforms the material from solid to vapor, and is friendly with the surroundings. Thus, there is no need for a waste gas treatment, or for many expensive process tools. **Figure 8** illustrates a scanning electron microscopy (SEM) image of a fabricated sample etched by laser micromachining. The smooth machined surface has attracted attention, and has wide applications in the fields of polymers, metals, ceramics, glasses, crystals, insulators, composite materials, etc.[94] With the help of programmable mechanical motion devices, this highly flexible shape etching provides an enormous advantage. Certainly, the graphitization of the surface caused by the high temperature is a distinct drawback. However, this effect may be overlooked if there is no electrical connection, especially in silicon-based all-dielectric metamaterials.

3.2. Self-Assembly Method

Recently, actively tunable properties have become increasingly important in practical applications. In the study by Lan

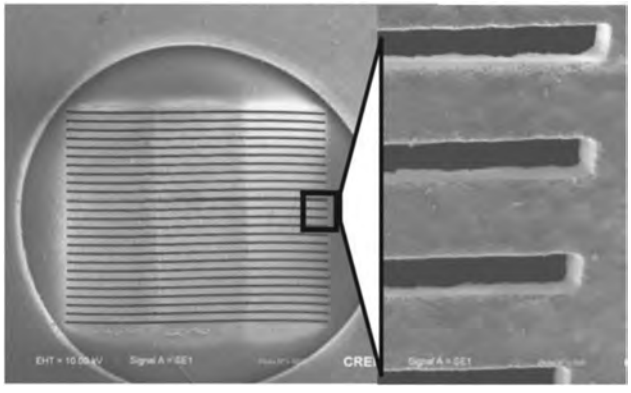

Figure 8. SEM image of a fabricated sample etched by laser micromachining. Reproduced with permission.[93] Copyright 2009, American Physical Society.

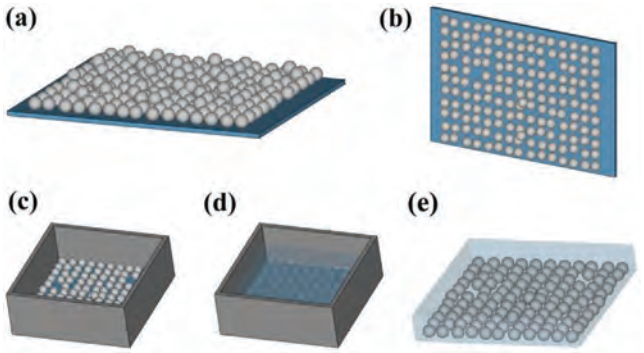

Figure 9. The process flow of the flexible all-dielectric metamaterials: a) attaching the ceramic particles by a tape, b) reversing and cleaning the tape for nearly single-layer metamaterials, c) loading the tape-based metamaterials on the container, d) casting the polydimethylsiloxane, and e) peeling the proposed metamaterials.

et al.,[95] a flexible all-dielectric metamaterials with single-layer ceramic microspheres embedded in an elastomeric medium led to new insights into the design and fabrication of all-dielectric metamaterials in the terahertz (THz) regime. In the study, spherical zirconia particles were prepared using an inorganic sol–gel process. During the fabrication of the proposed metamaterials, the key was embedding the particles into the elastomeric medium. The fabrication process is illustrated in **Figure 9**. First, a piece of tape, as shown in Figure 9a, was used to attach the prepared spherical particles. After reversing the tape, a nearly full single layer of metamaterials was obtained (Figure 9b). Then, the tape was placed on the bottom of a stainless steel container made by a traditional mechanical machining method (Figure 9c). For embedding in the elastomeric medium, the side of the tape with particles was faced toward the up direction, and then the polydimethylsiloxane polymer was cast into the container (Figure 9d). Finally, the proposed metamaterials were peeled off and obtained after 24 h of curing (Figure 9e).

Nowadays, the exiting fabrication methods for all-dielectric metamaterials often have difficulty in regards to the preparative scale, precision, and cost. To prepare large-scale, high-precision, and flexible ceramic microsphere all-dielectric metamaterials, our group has proposed a micro-template-assisted self-assembly (MTAS) method.[96] This method is inspired by nanotemplate-assisted self-assembly technology, and is shown in **Figure 10**. First, a thin stainless steel element with various geometries is etched using a solid-state laser. It is then used as the template in the MTAS method. An adhesive layer is employed to fix the microspheres and the template. After these preparations, the microspheres can be moved with the help of a soft slicker that blows the microspheres from left to right. Under the resultant force of the external force (F_e) and gravity (F_g), the microspheres are pushed and fixed in the holes of the template. Finally, a well-controlled microsphere-based all-dielectric metamaterial is obtained after removing the template and redundant microspheres. A fabricated sample as depicted in Figure 10b has a relatively regular shape. Owing to the flexibility of the geometries, the all-dielectric metamaterials can be designed to arbitrary patterns and scale, ensuring low-cost and environmentally friendly fabrication.

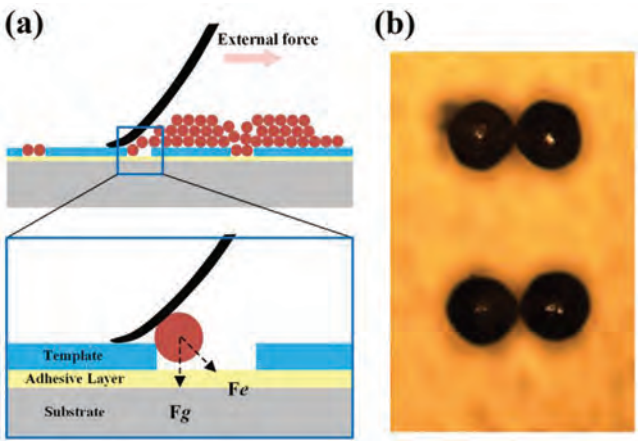

Figure 10. a) Illustration of the MTAS and b) a fabricated sample. Reproduced with permission.[96] Copyright 2019, Chinese Laser Press.

3.3. 3D Direct Writing Method

3D direct writing technology is a low-cost, easy-to-fabricate technology for all-dielectric metamaterials in the THz range.[40,97] Generally, $TbFeO_3$ is prepared as the ink of a 3D printer. In a deionized water solution of polyvinyl alcohol, $TbFeO_3$ inks are obtained by mixing Tb_4O_7 and pre-sintered Fe_2O_3 powders. To ensure thorough mixing and obtain well-distributed suspensions, a step-by-step addition of the Fe_2O_3 powders is employed, and 20–30 min of shaking is required in each step. Then, the prepared $TbFeO_3$ inks are loaded into a syringe connected with a three-axis motion element of the printer to build the desired metamaterial structures. A layer-by-layer process (as illustrated in **Figure 11**) is conducted to build the 3D metamaterial model based on a computer-aided fabrication program. After a conventional solid-state sintering process, the proposed all-dielectric metamaterial is obtained, and is ready for applications.

For a clear comparison, detailed information on the terahertz all-dielectric metamaterial fabrication methods, including laser micromachining, DRIE, the self-assembly method, and 3D direct writing, are listed in **Table 2**. These methods have their own inherent advantages and disadvantages. Laser machining prepares the material in a single step, saving a large amount of time in fabrication. The ability to operate simply has led laser direct writing to become a pretreatment for many

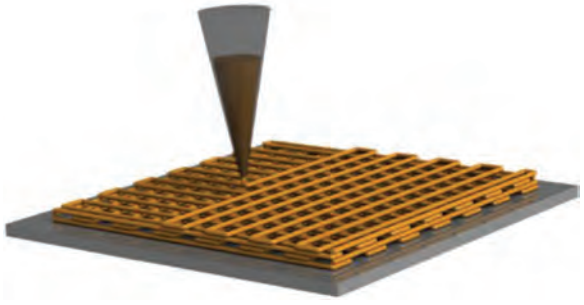

Figure 11. Schematic of the layer-by-layer 3D direct writing technique. Reproduced with permission.[97] Copyright 2018, Optical Society of America.

Table 2. Comparison of fabrication techniques for terahertz all-dielectric metamaterials.

Method	Material	Time consuming	Precision	Structure	Function	Ref.
Laser micromachining	$SrTiO_3$	No	μm	Rods	Negative effective permeability	[93]
	Ag	No	μm	Split ring	Improving electromagnetic property	[98]
	Metal film	No	μm	Wire grid	Low insertion losses	[99]
	Multilayer films	No	μm	Split ring	High throughput and efficiency	[100]
DRIE	Silicon	Yes	μm	Grating structure	High-quality magnetic resonances	[92]
	Silicon	Yes	μm	Square holes	THz photonic crystals	[101]
	Silicon	Yes	μm	Waveguides structure	Miniaturization	[102]
	Silicon	Yes	μm	Square array with disks	Dual-band and high absorption	[103]
Self-assembly	Zirconia	Yes	μm	Single layer	Tunable characteristic	[95]
	ZrO_2 and Al_2O_3	Yes	μm	Single layer	Broadband reflection	[96]
	Hybrid TiO_2	Yes	nm	Nanosphere coating	Enhancing diffuse reflectance	[104]
	Zirconia	Yes	μm	Diamond structure	Full photonic band gap	[105]
3D direct writing	$TbFeO_3$	Yes	μm	Woodpile	Polarization-independent refraction	[97]
	$TbFeO_3$	Yes	μm	Grating and face-centered cubic structure	Polarization-independent and deep transmittance	[40]
	Al_2O_3	Yes	μm	Woodpile	Flexible operating frequency	[106]
	$BaTiO_3$	Yes	μm	Periodic diamond	Modulating refractive indices	[107]

methods. Other prominent merits include its high efficiency, high speed, high precision, low cost, and wide usage.[98–100] However, laser cauterization causes great harm to the materials. Moreover, the fabricated pattern is usually 2D. Thus, this method is often used to fabricate various surface structures. Among them, the periodic grating and split ring are commonly designed for improving the electromagnetic performance of terahertz devices. The DRIE technology features a vertical aspect ratio, high precision, high etched rates, and anisotropic profiles.[101–103] Many silicon-based devices have been fabricated by this method, owing to the resultant high absorption, high-quality resonance, dual-bands, and miniaturization. A PR or metal can act as the mask in DRIE. However, the reaction between the metal and gas results in burrs on the bottom. The DRIE technology is not suitable for the fabrications of complex 3D structures, such as spheres. Moreover, the precision depends on the etching rates, gas flow, and pressure. The post-processing also requires a significant amount of time.

The proposal of the self-assembly method aims at processing sphere-based metamaterials. The prominent merits of this proposal include its large-scale, low intrinsic loss, high precision, and flexibility. These merits have been applied in hybrid microstructures and high-quality THz all-dielectric metamaterials for enhancing the diffuse reflectance, providing broadband reflection, and gaining tunable characteristics.[104,105] Owing to its strong pertinence to specific applications, the application range of this method is limited. In addition, the requirements for a ceramic microsphere, container, and template will increase the complexity of the fabrication. Regarding the fabrication of a 3D structure, 3D direct writing technology can be an effective approach. The multilayer structure, flexible shape, and automatic control make this method an alluring fabrication technique. Owing to the direct formation, no waste material will be generated. Here, $TbFeO_3$, Al_2O_3, and $BaTiO_3$ were adapted to design periodic structures for flexible tunable THz devices.[106,107] Nevertheless, many limitations restrict its applications, including the syringe blocking, flow speed, and pressure. The preparation of inks and final solid-state sintering process requires the most time.

4. Optical All-Dielectric Metamaterial Fabrication Techniques

During the past few years, optical all-dielectric metamaterials and metasurfaces have become a popular research issue in the field of nanophotonics.[108–115] This can be attributed to their low loss, special photonic modes, and good compatibility.[116–122] However, fabricating all-dielectric all-dielectric metamaterials still involves challenges. Up to now, various fabrication methods have been proposed for obtaining all-dielectric metamaterials. Here, we review these methods, and point out their advantages and disadvantages.

4.1. Lithography Method

In recent years, the most widely used method for optical all-dielectric metamaterials is called the electron-beam lithography method. The wide usage can be attributed to the considerable advantages of the electron-beam lithography method. For example, as a standard and widely used micro/nanofabrication processing technique, the electron-beam lithography method has several properties, such as good precision, good repeatability, and high reliability. Using this method, considerable all-dielectric metamaterials can be obtained.

The most simple and straightforward process for the fabrication of all-dielectric metamaterials using electron-beam

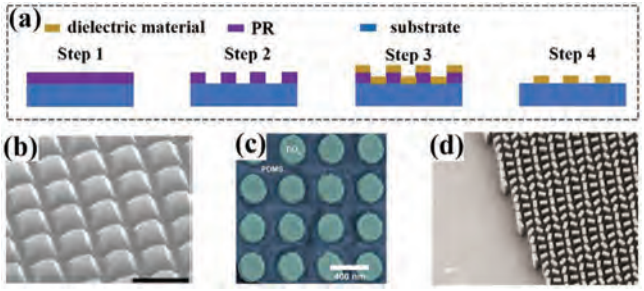

Figure 12. a) Fabrication process of all-dielectric metamaterial using "lift-off" process method. b) Photograph of a color printer. Reproduced with permission.[123] Copyright 2017, American Chemical Society. c) Photograph of a flexible all-dielectric metamaterial. Reproduced with permission.[124] Copyright 2015, American Chemical Society. d) Photograph of a metalenses. Reproduced with permission.[125] Copyright 2016, American Association for the Advancement of Science.

lithography is called a "lift-off" process. The schematic flow for this method is shown in **Figure 12**a. First, a PR film is deposited on a substrate (glass or quartz). Then, the electron-beam lithography is applied to the PR film. After that, the target dielectric material is deposited on it. Usually, the deposition method includes magnetron sputtering, electron-beam evaporation, and atomic layer deposition. Finally, the all-dielectric metamaterials are obtained after removing the PR film. This method has been used to fabricate all-dielectric metasurfaces, such as color metasurfaces[123] (Figure 12b), flexible all-dielectric metamaterials[124] (Figure 12c), metalenses[125] (Figure 12d), and absorbers.[126] However, this method has several evident disadvantages. For example, the thickness of dielectric film is limited, and the fabricated particles are usually trapezoidal. In addition, in the deposition of the dielectric film, the PR can suffer from deformations, owing to the temperature. Up to now, this method has been employed to fabricate TiO_2 and Si all-dielectric metamaterials.

In fact, a combination of the electron-beam lithography method with reactive-ion etching is the most widely used approach in the fabrication of all-dielectric metamaterials. The schematic flow for this method is provided in **Figure 13**a. First,

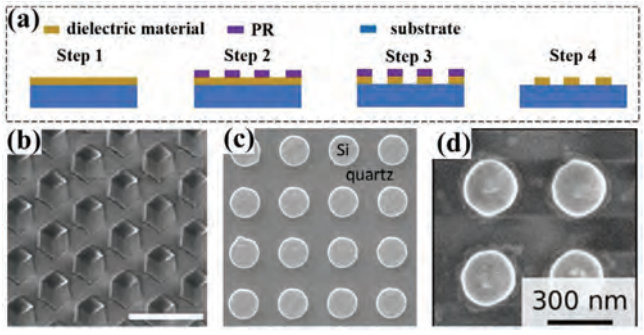

Figure 13. a) Fabrication process of all-dielectric metamaterial using the combination of electron-beam lithography method with reactive-ion etching. b) Optical magnetism from tellurium array. Reproduced with permission.[127] Copyright 2012, American Physical Society. c) Biosensing from silicon nanodisk array. Reproduced with permission.[128] Copyright 2017, American Chemical Society. d) Ultrafast all-optical switching from silicon nanodisk array. Reproduced with permission.[131] Copyright 2015, American Chemical Society.

the dielectric material film is deposited on the substrate. After that, the electron-beam lithography is applied to the PR film. Then, a reactive-ion etching process is employed to etch the exposed dielectric film. After that, the all-dielectric metamaterials are obtained after removing the PR film. As compared to the "lift-off" process, this method can avoid the disadvantages mentioned above. As a result, nearly 90% of the reported all-dielectric metamaterials are fabricated using this method.[127–133] Figure 13b–d shows examples of properties from all-dielectric metamaterials fabricated using this method, including optical magnetism from a tellurium array,[127] biosensing from a silicon nanodisk array,[128] and ultrafast all-optical switching from a silicon nanodisk array.[131] It should be noted that although the electron-beam lithography method has considerable advantages such as good precision, high reliability, and good repeatability, it still suffers from disadvantages including its limited area, expensive cost, and complicated time-consuming process. In addition, this method can only fabricate 2D elements, and cannot fabricate flexible all-dielectric metamaterials.[134–141]

4.2. Laser Method

As mentioned above, the lithography method for all-dielectric metamaterials usually suffers from excessive time consumption and price. Thus, a fast fabrication method is highly desired. Femtosecond laser is often used to prepare microstructures owing to its unique properties such as high precision and low time consumption. A laser-assisted method has been proven to fabricate nanoparticles with diameters of ≈100 nm. In addition, the laser-assisted method has several advantages, such as its high resolution and high energy density, as well as being material-free. Consequently, it is not surprising that this method has become a promising fabrication method for high-quality all-dielectric metamaterials. There are several approaches to fabricating all-dielectric metamaterials or all-dielectric resonators using the laser-assisted method. The two most representative approaches are direct laser ablation and laser-induced transfer.

In the process of direct laser ablation, fragmentation made of the target material is converted into spherical nanoparticles by using ultrashort laser pulses, and then the spherical nanoparticles are deposited on the substrate. This method has been proven to fabricate single-crystalline nanoparticles. Mie resonances of the all-dielectric nanoparticle resonators have also been demonstrated (**Figure 14**a).[142] The advantages of this method are evident. For example, high temperatures and/or a vacuum are not required. In addition, these all-dielectric resonators can support high-quality-factor resonances. However, the disadvantages are also evident, as it is difficult to control the size and location. Laser-induced transfer is a promising laser-assisted method as compared to direct laser ablation. In this method, a transparent donor substrate (glass or quartz) is placed on the dielectric material substrate (silicon) with a space. The laser radiation focuses on the interface between the dielectric material substrate and donor substrate. The fragmentation made of the dielectric material is converted into spherical nanoparticles, and is deposited on the transparent donor substrate (Figure 14b).[143] There are several advantages to this method. For example, the all-dielectric resonators can be tailored, and

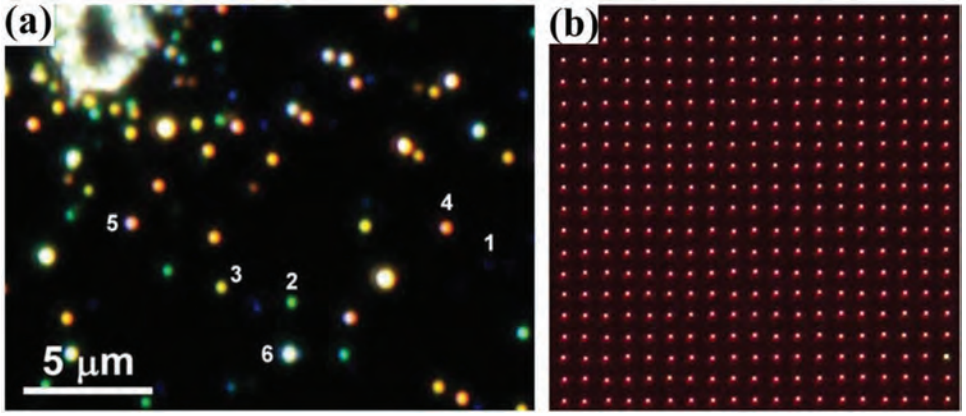

Figure 14. All-dielectric resonators fabricated by laser method. a) Silicon nanoparticles made by direct laser ablation. Reproduced with permission.[142] Copyright 2012, Springer Nature. b) Silicon nanoparticles made by laser-induced transfer. Reproduced with permission.[143] Copyright 2014, Springer Nature.

placed with high precision. Furthermore, this method is available for nearly all semiconductor materials and dielectric materials.

4.3. Nanosphere Lithography

The nanosphere lithography method is a special nanoparticle fabrication technology for fabricating high-quality and uniform single layers of nanoparticles, with sizes ranging from 100 nm to 1 μm. In addition, this method can solve the problems regarding high cost and complexity. More importantly, large-scale single-layer nanoparticles can be obtained using this method.

In recent decades, considerable research groups have demonstrated that the nanosphere lithography method can be employed to fabricate various single-layer arrayed nanoparticles. As a result, it has been naturally extended to the fabrication of all-dielectric metamaterials. Several research groups have demonstrated that high-quality and large-scale all-dielectric metamaterials can be easily fabricated using this method.[144,145] Using this method, our group demonstrated a flexible, all-dielectric metasurface, and found its potential applications in sensing.[145] **Figure 15**a shows the

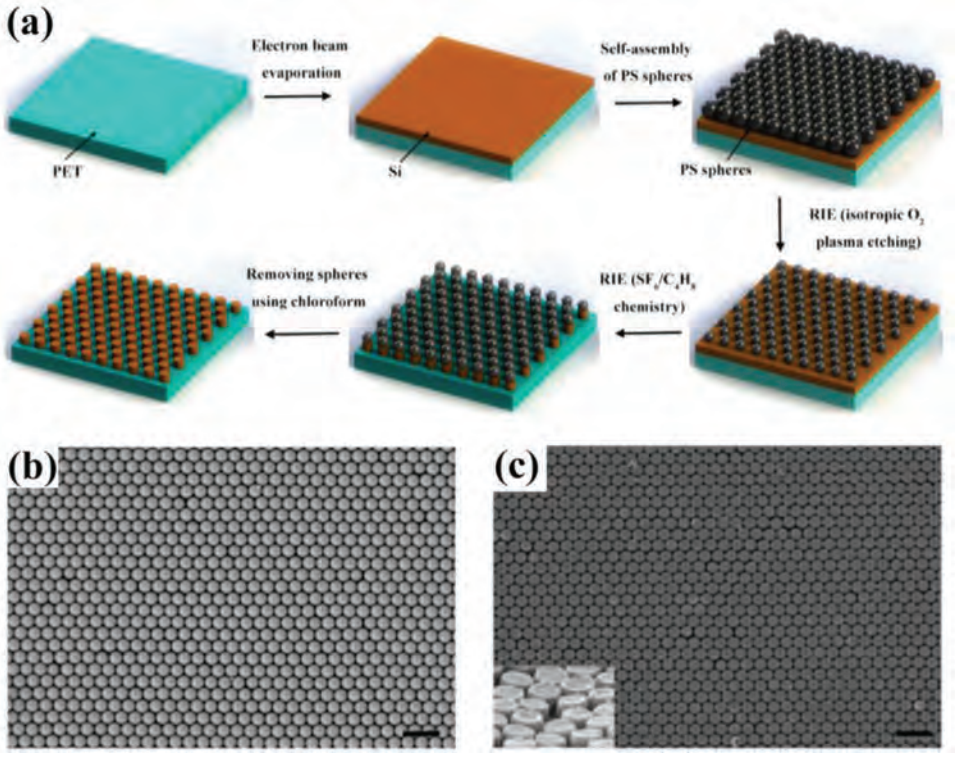

Figure 15. a) Fabrication process of all-dielectric metamaterial using nanosphere lithography method. b) SEM photograph of single PS spheres. c) SEM photograph of fabricated all-dielectric metamaterials. Reproduced with permission.[145] Copyright 2017, Optical Society of America.

fabrication process of an all-dielectric metamaterial using the nanosphere lithography method. First, a dielectric material film is deposited on the target substrate (transparent substrate) using electron beam evaporation. After that, a single layer of compactly arrayed PS spheres is self-assembled at the air/water interface. Then, the single layer of PS spheres is transferred to the dielectric film/substrate, to function as a mask (Figure 15b). To achieve the desired patterns, a reactive ion etching process is used to shrink the size of the PS spheres. Next, the etching process is employed to remove the exposed Si film. Finally, a flexible, all-dielectric metasurface is obtained after removing the PS spheres (Figure 15c). Notably, although this method can fabricate large-scale all-dielectric metamaterials with low cost and a simple fabrication process, it still suffers from some drawbacks. For example, the patterns for the fabricated all-dielectric metamaterials are seriously limited. In addition, it is difficult to obtain all-dielectric metamaterials with an area exceeding 1 cm^2, and the process stability is poor. As a result, this method is still in the stages of laboratory research.

4.4. Chemistry Method

The chemistry method is a promising fabrication method for high-throughput all-dielectric metamaterials. An all-dielectric metamaterial based on a monodispersed silicon colloid is fabricated via the decomposition of trisilane in supercritical *n*-hexane under high-temperature condition.[146] In this fabrication, one can control the silicon colloid size by changing the reaction temperature and trisilane concentration. However, this method still has some disadvantages, such as high temperatures, high pressures, and inflammable gases.

Recently, Cho et al. reported an interesting study on fabricating high-throughput all-dielectric selenium-based metamaterials.[147] A scalable and versatile synthesis method was proposed. The synthetic process for the c-Se all-dielectric metamaterial can be seen in **Figure 16**a, where the selenous acid is reduced to c-Se colloids in the presence of a reducing agent at a temperature of 65 °C. The sodium salts of the naphthalene sulfonate formaldehyde condensate and hydroquinone are the reducing agents. In the synthetic process, the colloid uniformity and the solvent polarity can be controlled using water and ethylene glycol. Through the synthetic process, high-throughput dielectric colloidal nanoparticles can be prepared, without excessive cost and complex steps. With proper optimization, uniform dielectric colloidal nanoparticles can be obtained, as shown in Figure 16b. The authors have demonstrated that these nanoparticles support remarkable Mie resonances. In addition, these dielectric colloidal resonators can be easily self-assembled into versatile metaoptics systems.

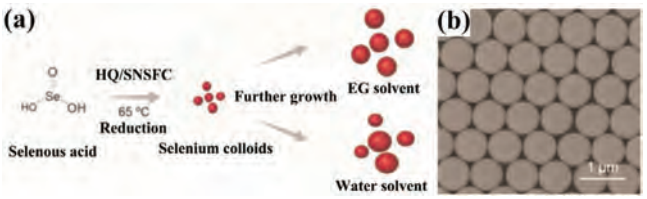

Figure 16. a) Synthetic route and b) SEM image of fabricated Se-based all-dielectric metamaterial. Reproduced with permission.[147] Copyright 2018, Wiley-VCH.

Table 3 provides a comparison of the fabrication techniques for optical all-dielectric metamaterials. It can be seen that each method has advantages and disadvantages. Usually, it is difficult to reach a balance between the time consumption, area, precision, price, and pattern. Owing to advantages, such as good precision, good repeatability, and high reliability, the electron-beam lithography method has been widely used. However, the cost is very high, and the fabrication area is limited. The laser method is a convenient method for high-quality all-dielectric metamaterials. However, the limited area and high cost remain outstanding problems. Several methods have been proposed to solve these problems, such as nanosphere lithography and the chemistry method. Using these methods, large-scale all-dielectric metamaterials can be obtained. In addition, the cost can be greatly reduced. However, the existing drawbacks, such as the relatively low precision and limited patterns, are evident. Recently, some other methods such as the focused ion beam (FIB), dewetting, and nanoimprint methods have been proposed.[148–150] For example, FIB method has been employed to obtain organometallic perovskite metasurfaces and chiral metamaterials. The dewetting methods have also been proposed to prepare the monocrystalline silicon-based Mie resonators. It is worth mentioning that nanoimprint method is a promising method for all-dielectric metamaterials (especially for practical applications), owing to its high precision, low cost, good repeatability, and high reliability.

Table 3. Comparison of fabrication techniques for optical all-dielectric metamaterials.

Method	Time consuming	Area	Precision	Price	Pattern	Ref.
Lithography method	Yes	Limited	High	High	Free	[123–141]
Direct laser ablation	No	Limited	Low	Moderate	Limited	[142]
Laser-induced transfer	No	Limited	High	Moderate	Limited	[143]
Nanosphere lithography	No	Large	Moderate	Low	Limited	[144,145]
Chemistry method	Yes	Large	Low	Low	Limited	[146,147]
FIB	No	Limited	High	High	Free	[148]
Dewetting	No	Large	Low	Low	Uncontrollable	[149]
Nanoimprint	No	Large	High	Low	Free	[150]

5. Summary and Outlook

Owing to its special properties such as low loss and good complementary metal oxide semiconductor compatibility,[151,152] there was little doubt that all-dielectric metamaterials would play a vital role in next generation of terahertz and photonic devices. Appropriate fabrication techniques could expand the applications of all-dielectric metamaterials.[153] However, until now, nearly all the reported all-dielectric metamaterials have remained in the laboratory stage.[154–156] To apply these metamaterials in practice, proper fabrication techniques become particularly important. This review provides a comprehensive overview of the available fabrication techniques for the realization of all-dielectric metamaterials. The currently developed fabrication techniques allow for production of different types of all-dielectric metamaterials based on various materials. The advantages and disadvantages of each fabrication method are presented.

As for the microwave all-dielectric metamaterials, the corresponding fabrication methods are relatively mature technologies. In addition, 3D printing is a promising method for the microwave all-dielectric metamaterials with a better performance. It is environmentally friendly and low cost. In theory, any material can be formed by this method, as long as the corresponding powder sample is obtained. For terahertz and optical all-dielectric metamaterials, most of the fabrication methods suffer from several difficulties, and require further development and improvement. It is worth mentioning that nanoimprint method is a promising method for terahertz and optical all-dielectric metamaterials (especially for practical applications), owing to its high precision, low cost, good repeatability, and high reliability.

Fabricating large-area all-dielectric metamaterials with low-cost and high precision is a significant challenge, especially for optical all-dielectric metamaterials. As a result, the use of a proper fabrication method in the corresponding frequency range is of great importance. In addition, a cost-effective method is highly desired when these all-dielectric metamaterials are applied in practice. Furthermore, the existing fabrication techniques for all-dielectric metamaterials with good flexibility and biological compatibility are promising, and need to be further developed. Understanding this information makes it easier to design all-dielectric metamaterials with desired properties.

Acknowledgements

This work was supported by the National Natural Science Foundation of China (grant nos. 51972033, 61774020, 61905021, 51788104, and 61672108), Beijing Youth Top-Notch Talent Support Program, Science and Technology Plan of Shenzhen City (grant nos. JCYJ20180306173235924 and JCYJ20180305164708625), and State Key Laboratory of Millimeter Waves (grant no. K202008).

Conflict of Interest

The authors declare no conflict of interest.

Keywords

all-dielectric metamaterials, fabrication techniques, microwaves, optical frequency, terahertz

Received: August 27, 2020
Revised: October 13, 2020
Published online:

[1] R. A. Shelby, D. R. Smith, S. Schultz, *Science* **2001**, *292*, 77.
[2] V. G. Veselago, *Phys.-Usp.* **1968**, *10*, 509.
[3] J. B. Pendry, A. J. Holden, D. J. Robbins, W. J. Stewart, *IEEE Trans. Microwave Theory Tech.* **1999**, *47*, 2075.
[4] J. B. Pendry, *Phys. Rev. Lett.* **2000**, *85*, 3966.
[5] J. B. Pendry, D. Schurig, D. R. Smith, *Science* **2006**, *312*, 1780.
[6] S. Anantha Ramakrishna, *Rep. Prog. Phys.* **2005**, *68*, 449.
[7] N. I. Landy, S. Sajuyigbe, J. J. Mock, D. R. Smith, W. J. Padilla, *Phys. Rev. Lett.* **2008**, *100*, 207402.
[8] D. R. Smith, W. J. Padilla, D. C. Vier, S. C. Nemat-Nasser, S. Schultz, *Phys. Rev. Lett.* **2000**, *84*, 4184.
[9] A. Boltasseva, V. M. Shalaev, *Metamaterials* **2008**, *2*, 1.
[10] Q. Zhao, L. Kang, B. Du, B. Li, J. Zhou, H. Tang, X. Liang, B. Zhang, *Appl. Phys. Lett.* **2007**, *90*, 3.
[11] J. Yao, Z. Liu, Y. Liu, Y. Wang, C. Sun, G. Bartal, A. M. Stacy, X. Zhang, *Science* **2008**, *321*, 930.
[12] J. B. Khurgin, *Nat. Nanotechnol.* **2015**, *10*, 2.
[13] P. R. West, S. Ishii, G. V. Naik, N. K. Emani, V. M. Shalaev, A. Boltasseva, *Laser Photonics Rev.* **2010**, *4*, 795.
[14] Y. F. Yu, A. Y. Zhu, R. Paniagua-Domínguez, Y. H. Fu, B. Luk'yanchuk, A. I. Kuznetsov, *Laser Photonics Rev.* **2015**, *9*, 412.
[15] M. I. Shalaev, J. Sun, A. Tsukernik, A. Pandey, K. Nikolskiy, N. M. Litchinitser, *Nano Lett.* **2015**, *15*, 6261.
[16] C. Y. Yang, J. H. Yang, Z. Y. Yang, Z. X. Zhou, M. G. Sun, V. E. Babicheva, K. P. Chen, *ACS Photonics* **2018**, *5*, 2596.
[17] Z. Huang, J. Wang, Z. Liu, G. Xu, Y. Fan, H. Zhong, B. Cao, C. Wang, K. Xu, *J. Phys. Chem. C* **2015**, *119*, 28127.
[18] P. Moitra, B. A. Slovick, Z. Gang Yu, S. Krishnamurthy, J. Valentine, *Appl. Phys. Lett.* **2014**, *104*, 171102.
[19] B. Slovick, Z. G. Yu, M. Berding, S. Krishnamurthy, *Phys. Rev. B* **2013**, *88*, 5514.
[20] P. Genevet, F. Capasso, F. Aieta, M. Khorasaninejad, R. Devlin, *Optica* **2017**, *4*, 139.
[21] R. C. Devlin, M. Khorasaninejad, W. T. Chen, J. Oh, F. Capasso, *Proc. Natl. Acad. Sci. USA* **2016**, *113*, 10473.
[22] R. T. Ako, A. Upadhyay, W. Withayachumnankul, M. Bhaskaran, S. Sriram, *Adv. Opt. Mater.* **2020**, *8*, 1900750.
[23] A. Ahmadi, H. Mosallaei, *Phys. Rev. B* **2008**, *77*, 045104.
[24] V. R. Tuz, V. V. Khardikov, A. S. Kupriianov, K. L. Domina, S. Xu, H. Wang, H. Sun, *Opt. Express* **2018**, *26*, 2905.
[25] H. J. Singh, A. Ghosh, *Nanoscale* **2018**, *10*, 16102.
[26] E. Semouchkina, R. Duan, G. Semouchkin, R. Pandey, *Sensors* **2015**, *15*, 9344.
[27] Q. Zhao, J. Zhou, F. Zhang, D. Lippens, *Mater. Today* **2009**, *12*, 60.
[28] I. W. Sudiarta, P. Chýlek, *Appl. Opt.* **2002**, *41*, 3545.
[29] C. Zhang, Y. Xu, J. Liu, J. Li, J. Xiang, H. Li, J. Li, Q. Dai, S. Lan, A. E. Miroshnichenko, *Nat. Commun.* **2018**, *9*, 2964.
[30] M. Decker, I. Staude, *J. Opt.* **2016**, *18*, 103001.
[31] K. Bi, Y. Guo, X. Liu, Q. Zhao, J. Xiao, M. Lei, J. Zhou, *Sci. Rep.* **2015**, *4*, 7001.
[32] C. Lan, K. Bi, J. Zhou, B. Li, *Appl. Phys. Lett.* **2015**, *107*, 211112.
[33] J. Sun, J. Zhou, B. Li, F. Kang, *Appl. Phys. Lett.* **2011**, *98*, 101901.

[34] R. Wang, J. Zhou, C. Q. Sun, L. Kang, Q. Zhao, J. B. Sun, *Prog. Electromagn. Res. Lett.* **2009**, *10*, 145.
[35] S. J. Corbitt, M. Francoeur, B. Raeymaekers, *J. Quant. Spectrosc. Radiat. Transfer* **2015**, *158*, 3.
[36] P. Cheben, R. Halir, J. H. Schmid, H. A. Atwater, D. R. Smith, *Nature* **2018**, *560*, 565.
[37] K. Cai, J. Sun, Q. Li, R. Wang, B. Li, J. Zhou, *Appl. Phys. A: Mater. Sci. Process.* **2011**, *102*, 501.
[38] S. Liu, J. F. Ihlefeld, J. Dominguez, E. F. Gonzales, J. Eric Bower, D. Bruce Burckel, M. B. Sinclair, I. Brener, *Appl. Phys. Lett.* **2013**, *102*, 161905.
[39] A. Khavasi, L. Chrostowski, Z. Lu, R. Bojko, *IEEE Photonics Technol. Lett.* **2016**, *28*, 2787.
[40] X. Zeng, R. Wang, X. Xi, B. Li, J. Zhou, *Appl. Phys. Lett.* **2018**, *113*, 081901.
[41] R. Yahiaoui, U. C. Chung, C. Elissalde, M. Maglione, V. Vigneras, P. Mounaix, *Appl. Phys. Lett.* **2012**, *101*, 042909.
[42] L. Li, J. Wang, J. Wang, H. Du, H. Huang, J. Zhang, S. Qu, Z. Xu, *Appl. Phys. Lett.* **2015**, *106*, 212904.
[43] L. Li, J. Wang, J. Wang, H. Ma, H. Du, J. Zhang, S. Qu, Z. Xu, *Sci. Rep.* **2016**, *6*, 24178.
[44] C. Lan, K. Bi, B. Li, X. Cui, J. Zhou, Q. Zhao, *Opt. Express* **2013**, *21*, 29592.
[45] L. Peng, L. Ran, H. Chen, H. Zhang, J. A. Kong, T. M. Grzegorczyk, *Phys. Rev. Lett.* **2007**, *98*, 157403.
[46] T. Lepetit, É. Akmansoy, J. P. Ganne, *Appl. Phys. Lett.* **2009**, *95*, 121101.
[47] T. Huang, Y. Lai, T. Yen, *Appl. Phys. Express* **2016**, *9*, 012003.
[48] J. Sun, X. Liu, J. Zhou, Z. Kudyshev, N. M. Litchinitser, *Sci. Rep.* **2015**, *5*, 16154.
[49] M. Lei, N. Feng, Q. Wang, Y. Hao, S. Huang, K. Bi, *J. Appl. Phys.* **2016**, *119*, 244504.
[50] K. Bi, W. Zhu, M. Lei, J. Zhou, *Appl. Phys. Lett.* **2015**, *106*, 173507.
[51] L. Li, J. Wang, H. Ma, J. Wang, M. Feng, H. Du, M. Yan, J. Zhang, S. Qu, Z. Xu, *Appl. Phys. Lett.* **2016**, *108*, 122902.
[52] J. Zhao, S. Wei, C. Wang, K. Chen, B. Zhu, T. Jiang, Y. Feng, *Opt. Express* **2018**, *26*, 8522.
[53] Y. J. Yoo, S. Ju, S. Y. Park, Y. Ju Kim, J. Bong, T. Lim, K. W. Kim, J. Y. Rhee, Y. Lee, *Sci. Rep.* **2015**, *5*, 14018.
[54] D. J. Gogoi, N. S. Bhattacharyya, *J. Appl. Phys.* **2017**, *122*, 175106.
[55] J. Xie, S. Quader, F. Xiao, C. He, X. Liang, J. Geng, R. Jin, W. Zhu, I. D. Rukhlenko, *IEEE Antennas Wireless Propag. Lett.* **2019**, *18*, 536.
[56] J. Xie, W. Zhu, I. D. Rukhlenko, F. Xiao, C. He, J. Geng, X. Liang, R. Jin, M. Premaratne, *Opt. Express* **2018**, *26*, 5052.
[57] I. V. Stenishchev, A. A. Basharin, *Sci. Rep.* **2017**, *7*, 9468.
[58] X. Huang, H. Yang, Z. Shen, J. Chen, H. Lin, Z. Yu, *J. Phys. D: Appl. Phys.* **2017**, *50*, 385304.
[59] Z. Wu, X. Chen, Z. Zhang, L. Heng, S. Wang, Y. Zou, *Appl. Phys. Express* **2019**, *12*, 057003.
[60] J. G. Huddleston, A. E. Visser, W. M. Reichert, H. D. Willauer, G. A. Broker, R. D. Rogers, *Green Chem.* **2001**, *3*, 156.
[61] A. R. Polu, H. Rhee, *Int. J. Hydrogen Energy* **2017**, *42*, 7212.
[62] R. Thangavel, A. G. Kannan, R. Ponraj, V. Thangavel, D. Kim, Y. Lee, *J. Power Sources* **2018**, *383*, 102.
[63] R. A. Sheldon, R. M. Lau, M. J. Sorgedrager, F. van Rantwijk, K. R. Seddon, *Green Chem.* **2002**, *4*, 147.
[64] M. J. Earle, J. M. S. S. Esperança, M. A. Gilea, J. N. Canongia Lopes, L. P. N. Rebelo, J. W. Magee, K. R. Seddon, J. A. Widegren, *Nature* **2006**, *439*, 831.
[65] J. L. Manzoori, M. Amjadi, J. Abulhassani, *Talanta* **2009**, *77*, 1539.
[66] J. Shin, W. A. Henderson, S. Passerini, *Electrochem. Commun.* **2003**, *5*, 1016.
[67] J. Gong, F. Yang, Q. Shao, X. He, X. Zhang, S. Liu, L. Tang, Y. Deng, *RSC Adv.* **2017**, *7*, 41980.
[68] E. Yang, F. Yang, J. Pei, X. Zhang, S. Liu, Y. Deng, *J. Phys. D: Appl. Phys.* **2019**, *52*, 395501.
[69] H. F. Ma, T. J. Cui, *Nat. Commun.* **2010**, *1*, 124.
[70] H. F. Ma, T. J. Cui, *Nat. Commun.* **2010**, *1*, 21.
[71] L. Zhang, H. K. H. Li, M. S. Tse, O. K. Tan, E. Chua, C. L. Chow, C. K. Lim, K. See, *Mater. Res. Bull.* **2017**, *96*, 164.
[72] D. Wang, T. Zhou, J. Zha, J. Zhao, C. Shi, Z. Dang, *J. Mater. Chem. A* **2013**, *1*, 6162.
[73] L. M. Clayton, A. K. Sikder, A. Kumar, M. Cinke, M. Meyyappan, T. G. Gerasimov, J. P. Harmon, *Adv. Funct. Mater.* **2005**, *15*, 101.
[74] W. Kim, S. Kim, *Appl. Surf. Sci.* **2015**, *329*, 219.
[75] C. Pecharroman, F. Esteban-Betegon, J. F. Bartolome, S. Lopez-Esteban, J. S. Moya, *Adv. Mater.* **2001**, *13*, 1541.
[76] F. Liang, L. Zhang, W. Lu, Q. Wan, G. Fan, *Appl. Phys. Lett.* **2016**, *108*, 072902.
[77] Y. Chen, Y. Wang, H. Zhang, X. Li, C. Gui, Z. Yu, *Carbon* **2015**, *82*, 67.
[78] G. Subodh, V. Deepu, P. Mohanan, M. T. Sebastian, *Appl. Phys. Lett.* **2009**, *95*, 062903.
[79] J. Zha, T. Zhu, Y. Wu, S. Wang, R. K. Li, Z. Dang, *J. Mater. Chem. C* **2015**, *3*, 7195.
[80] P. Xie, Z. Wang, Z. Zhang, R. Fan, C. Cheng, H. Liu, Y. Liu, T. Li, C. Yan, N. Wang, Z. Guo, *J. Mater. Chem. C* **2018**, *6*, 5239.
[81] C. Li, D. Liu, D. Dai, *Nanophotonics* **2019**, *8*, 227.
[82] A. B. Evlyukhin, S. M. Novikov, U. Zywietz, R. L. Eriksen, C. Reinhardt, S. I. Bozhevolnyi, B. N. Chichkov, *Nano Lett.* **2012**, *12*, 3749.
[83] I. Staude, A. E. Miroshnichenko, M. Decker, N. T. Fofang, S. Liu, E. Gonzales, J. Dominguez, T. S. Luk, D. N. Neshev, I. Brener, Y. Kivshar, *ACS Nano* **2013**, *7*, 7824.
[84] S. Jahani, Z. Jacob, *Nat. Nanotechnol.* **2016**, *11*, 23.
[85] W. Tian, H. Sun, L. Chen, P. Wangyang, X. Chen, J. Xiong, L. Li, *InfoMat* **2019**, *1*, 140.
[86] Z. J. Ma, S. M. Hanham, P. Albella, B. Ng, H. T. Lu, Y. D. Gong, S. A. Maier, M. H. Hong, *ACS Photonics* **2016**, *3*, 1010.
[87] J. A. Bossard, X. T. Liang, L. Li, S. Yun, D. H. Weiner, T. S. Mayer, P. F. Cristman, A. Diaz, I. C. Khoo, *IEEE Antennas Wireless Propag. Lett.* **2008**, *56*, 1308.
[88] S. G. Park, K. Lee, D. Han, J. Ahn, K. H. Jeong, *Appl. Phys. Lett.* **2014**, *105*, 091101.
[89] Y. J. Zhao, B. W. Li, C. W. Lan, K. Bi, Z. W. Qu, *Opt. Express* **2017**, *25*, 22158.
[90] D. C. Wang, S. Sun, Z. Feng, W. Tan, C. W. Qiu, *Appl. Phys. Lett.* **2018**, *113*, 201103.
[91] K. B. Fan, J. Y. Suen, X. Y. Liu, W. J. Padilla, *Optica* **2017**, *4*, 601.
[92] C. W. Lan, H. Ma, M. T. Wang, Z. H. Gao, K. Liu, K. Bi, J. Zhou, X. J. Xin, *ACS Appl. Mater. Interfaces* **2019**, *11*, 14229.
[93] H. Němec, P. Kužel, F. Kadlec, C. Kadlec, R. Yahiaoui, P. Mounaix, *Phys. Rev. B* **2009**, *79*, 241108.
[94] K. M. Ahmmed, C. Grambow, A. M. Kietzig, *Micromachines* **2014**, *5*, 1219.
[95] C. W. Lan, K. Bi, B. W. Li, Y. J. Zhao, Z. W. Qu, *Opt. Express* **2017**, *25*, 29155.
[96] K. Bi, D. Q. Yang, J. Chen, Q. M. Wang, H. Y. Wu, C. W. Lan, Y. P. Yang, *Photonics Res.* **2019**, *7*, 457.
[97] X. X. Zeng, R. Wang, X. Q. Xi, B. Li, J. Zhou, *Opt. Express* **2018**, *26*, 17056.
[98] Z. C. Chen, N. R. Han, Z. Y. Pan, Y. D. Gong, T. C. Chong, M. H. Hong, *Opt. Mater. Express* **2011**, *1*, 151.
[99] N. Born, R. Gente, I. Al-Naib, M. Koch, *Electron. Lett.* **2015**, *51*, 1012.
[100] M. L. Tseng, P. C. Wu, S. Sun, C. M. Chang, W. T. Chen, C. H. Chu, P. L. Chen, L. Zhou, D. W. Huang, T. J. Yen, D. P. Tsai, *Laser Photonics Rev.* **2012**, *6*, 702.
[101] N. Jukam, M. S. Sherwin, *Appl. Phys. Lett.* **2003**, *83*, 21.

[102] C. Jung, T. J. Reck, J. V. Siles, R. Lin, C. Lee, J. Gill, K. Cooper, I. Mehdi, G. Chattopadhyay, *IEEE Trans. Terahertz Sci. Technol.* **2016**, *6*, 690.
[103] Y. Wang, D. Y. Zhu, Z. J. Cui, L. Hou, L. Lin, F. F. Qu, X. X. Liu, P. C. Nie, *ACS Omega* **2019**, *4*, 18645.
[104] H. Lu, M. Huang, K. S. Shen, J. Zhang, S. Q. Xia, C. Dong, Z. G. Xiong, T. Zhu, D. P. Wu, B. Zhang, X. Z. Zhang, *Nanoscale Res. Lett.* **2018**, *13*, 328.
[105] K. Takagi, A. Kawasaki, *Appl. Phys. Lett.* **2009**, *94*, 021110.
[106] C. R. Tubio, J. A. Novoa, J. Martin, F. Guitian, J. R. Salgueiro, A. Gil, *RCS Adv.* **2016**, *6*, 2450.
[107] P. F. Zhu, W. Y. Yang, R. Wang, S. Gao, B. Li, Q. Li, *Adv. Opt. Mater.* **2017**, *5*, 1600977.
[108] S. Jahani, S. Kim, J. Atkinson, J. C. Wirth, F. Kalhor, A. A. Noman, W. D. Newman, P. Shekhar, K. Han, V. Van, R. G. DeCorby, L. Chrostowski, M. Qi, Z. Jacob, *Nat. Commun.* **2018**, *9*, 1893.
[109] A. E. Krasnok, A. B. Evlyukhin, B. N. Chichkov, D. G. Baranov, D. A. Zuev, O. V. Kotov, S. I. Lepeshov, *Optica* **2017**, *4*, 814.
[110] E. Kallos, I. Chremmos, V. Yannopapas, *Phys. Rev. B* **2012**, *86*, 245108.
[111] X. Luo, D. Tsai, M. Gu, M. Hong, *Chem. Soc. Rev.* **2019**, *48*, 2458.
[112] N. Yu, F. Capasso, *Nat. Mater.* **2014**, *13*, 139.
[113] M. Khorasaninejad, F. Aieta, P. Kanhaiya, M. A. Kats, P. Genevet, D. Rousso, F. Capasso, *Nano Lett.* **2015**, *15*, 5358.
[114] D. Lin, P. Fan, E. Hasman, M. L. Brongersma, *Science* **2014**, *345*, 298.
[115] O. Takayama, D. Artigas, L. Torner, *Nat. Nanotechnol.* **2014**, *9*, 419.
[116] C. Wu, N. Arju, G. Kelp, J. A. Fan, J. Dominguez, E. Gonzales, E. Tutuc, I. Brener, G. Shvets, *Nat. Commun.* **2014**, *5*, 3892.
[117] R. Sarma, D. de Ceglia, N. Nookala, M. A. Vincenti, S. Campione, O. Wolf, M. Scalora, M. B. Sinclair, M. A. Belkin, I. Brener, *ACS Photonics* **2019**, *6*, 1458.
[118] Q. Wei, B. Sain, Y. Wang, B. Reineke, X. Li, L. Huang, T. Zentgraf, *Nano Lett.* **2019**, *19*, 8964.
[119] Y. Hu, L. Li, Y. Wang, M. Meng, L. Jin, X. Luo, Y. Chen, X. Li, S. Xiao, H. Wang, Y. Luo, C. Qiu, H. Duan, *Nano Lett.* **2020**, *20*, 994.
[120] C. Gong, W. Liu, N. He, H. Dong, Y. Jin, S. He, *Nanoscale* **2019**, *11*, 1856.
[121] A. Forouzmand, H. Mosallaei, *Adv. Opt. Mater.* **2017**, *5*, 1700147.
[122] M. V. Gorkunov, O. Y. Rogov, A. V. Kondratov, V. V. Artemov, R. V. Gainutdinov, A. A. Ezhov, *Sci. Rep.* **2018**, *8*, 11623.
[123] S. Sun, Z. Zhou, C. Zhang, Y. Gao, Z. Duan, S. Xiao, Q. Song, *ACS Nano* **2017**, *11*, 4445.
[124] P. Gutruf, C. Zou, W. Withayachumnankul, M. Bhaskaran, S. Sriram, C. Fumeaux, *ACS Nano* **2016**, *10*, 133.
[125] M. Khorasaninejad, W. T. Chen, R. C. Devlin, J. Oh, A. Y. Zhu, F. Capasso, *Science* **2016**, *352*, 1190.
[126] C. Zou, P. Gutruf, W. Withayachumnankul, L. Zou, M. Bhaskaran, S. Sriram, C. Fumeaux, *Opt. Lett.* **2016**, *41*, 3391.
[127] J. C. Ginn, I. Brener, D. W. Peters, J. R. Wendt, M. B. Sinclair, *Phys. Rev. Lett.* **2012**, *108*, 097402.
[128] O. Yavas, M. Svedendahl, P. Dobosz, V. Sanz, R. Quidant, *Nano Lett.* **2017**, *17*, 4421.
[129] A. Krasnok, M. Caldarola, N. Bonod, A. Alú, *Adv. Opt. Mater.* **2018**, *6*, 1701094.
[130] M. Caldarola, P. Albella, E. Cortés, M. Rahmani, T. Roschuk, G. Grinblat, R. F. Oulton, A. V. Bragas, S. A. Maier, *Nat. Commun.* **2015**, *6*, 7915.
[131] M. R. Shcherbakov, P. P. Vabishchevich, A. S. Shorokhov, K. E. Chong, C. Duk-Yong, S. Isabelle, A. E. Miroshnichenko, D. N. Neshev, A. A. Fedyanin, Y. S. Kivshar, *Nano Lett.* **2015**, *15*, 6985.
[132] Y. Yang, I. I. Kravchenko, D. P. Briggs, J. Valentine, *Nat. Commun.* **2014**, *5*, 5753.
[133] K. E. Chong, B. Hopkins, I. Staude, A. E. Miroshnichenko, J. Dominguez, M. Decker, D. N. Neshev, I. Brener, Y. S. Kivshar, *Small* **2014**, *10*, 1985.
[134] S. Wang, P. C. Wu, V.-C. Su, Y.-C. Lai, M.-K. Chen, H. Y. Kuo, B. H. Chen, Y. H. Chen, T. T. Huang, J.-H. Wang, *Nat. Nanotechnol.* **2018**, *13*, 227.
[135] F. Zhang, M. Pu, X. Li, P. Gao, X. Ma, J. Luo, H. Yu, X. Luo, *Adv. Funct. Mater.* **2017**, *27*, 1704295.
[136] L. Huang, H. Mühlenbernd, X. Li, X. Song, B. Bai, Y. Wang, T. Zentgraf, *Adv. Mater.* **2015**, *27*, 6444.
[137] Z. Yang, Z. Wang, Y. Wang, X. Feng, M. Zhao, Z. Wan, L. Zhu, J. Liu, Y. Huang, J. Xia, *Nat. Commun.* **2018**, *9*, 4607.
[138] J. Tian, H. Luo, Q. Li, X. Pei, K. Du, M. Qiu, *Laser Photonics Rev.* **2018**, *12*, 1800076.
[139] B. Wang, F. Dong, Q.-T. Li, D. Yang, C. Sun, J. Chen, Z. Song, L. Xu, W. Chu, Y.-F. Xiao, *Nano Lett.* **2016**, *16*, 5235.
[140] Y. Nagasaki, M. Suzuki, J. Takahara, *Nano Lett.* **2017**, *17*, 7500.
[141] Y. Horie, S. Han, J.-Y. Lee, J. Kim, Y. Kim, A. Arbabi, C. Shin, L. Shi, E. Arbabi, S. M. Kamali, *Nano Lett.* **2017**, *17*, 3159.
[142] A. I. Kuznetsov, A. E. Miroshnichenko, H. F. Yuan, J. Zhang, B. Luk'Yanchuk, *Sci. Rep.* **2012**, *2*, 492.
[143] U. Zywietz, A. B. Evlyukhin, C. Reinhardt, B. N. Chichkov, *Nat. Commun.* **2014**, *5*, 3402.
[144] P. Moitra, B. A. Slovick, W. Li, I. I. Kravchencko, D. P. Briggs, S. Krishnamurthy, J. Valentine, *ACS Photonics* **2015**, *2*, 692.
[145] G. Zhang, C. Lan, H. Bian, R. Gao, J. Zhou, *Opt. Express* **2017**, *25*, 22038.
[146] L. Shi, J. T. Harris, R. Fenollosa, I. Rodriguez, X. Lu, B. A. Korgel, F. Meseguer, *Nat. Commun.* **2013**, *4*, 1904.
[147] Y. Cho, J. H. Huh, K. Kim, S. Lee, *Adv. Opt. Mater.* **2019**, *7*, 1801167.
[148] B. Gholipour, G. Adamo, D. Cortecchia, H. N. S. Krishnamoorthy, M. D. Birowosuto, N. I. Zheludev, C. Soci, *Adv. Mater.* **2017**, *29*, 1604268.
[149] M. Abbarchi, M. Naffouti, B. Vial, A. Benkouider, L. Lermusiaux, L. Favre, A. Ronda, S. Bidault, I. Berbezier, N. Bonod, *ACS Nano* **2014**, *8*, 11181.
[150] S. V. Makarov, V. Milichko, E. V. Ushakova, M. Omelyanovich, A. Cerdan Pasaran, R. Haroldson, B. Balachandran, H. Wang, W. Hu, Y. S. Kivshar, *ACS Photonics* **2017**, *4*, 728.
[151] Z. Y. Zhou, X. Y. Shen, C. C. Fang, J. P. Huang, *ES Energy Environ.* **2019**, *6*, 85.
[152] K. Sun, L. Y. Wang, Z. X. Wang, X. F. Wu, G. H. Fan, Z. Y. Wang, C. B. Cheng, R. H. Fan, M. Y. Dong, Z. H. Guo, *Phys. Chem. Chem. Phys.* **2020**, *22*, 5114.
[153] J. N. Ni, R. Y. Zhan, J. Qiu, J. C. Fan, B. B. Dong, Z. H. Guo, *J. Mater. Chem. C* **2020**, *8*, 11748.
[154] T. Li, Y. Gao, K. Zheng, Y. M. Ma, D. Ding, H. Zhang, *ES Energy Environ.* **2019**, *5*, 102.
[155] J. M. Manimala, P. P. Kulkarni, K. Madhamshetty, *Adv. Compos. Hybrid Mater.* **2018**, *1*, 797.
[156] T. C. Lim, *Adv. Compos. Hybrid Mater.* **2019**, *2*, 657.

Ke Bi received his Ph.D. degree from the Nanjing University of Aeronautics and Astronautics in 2012. From 2012 to 2014, he was an assistant researcher at Tsinghua University. He is currently an associate professor at the Beijing University of Posts and Telecommunications. His research group focuses on information functional materials and devices, and electromagnetic metamaterials and devices.

Chuwen Lan received his Ph.D. degree from the Tsinghua University in 2017. From 2017 to 2019, he was a postdoctoral fellow at Beijing University of Posts and Telecommunications. He is currently a lecturer at Beijing University of Posts and Telecommunications. His research interests include metamaterials, THz technology, and optical communications.

Ming Lei received his Ph.D. degree from Institute of Physics, Chinese Academy of Science in 2007. He worked as a postdoctoral fellow at the Hong Kong University of Science and Technology and Chinese University of Hong Kong from 2007 to 2008 and from 2009 to 2010, respectively. He is now a professor at the Beijing University of Posts and Telecommunications. His research group focuses on synthesis of low-dimensional semiconductor and related photoelectric properties.